JOURNAL OF PROPULSION AND POWER
Vol. 29, No. 5, September–October 2013

CuO/Al Thermites for Solid Rocket Motor Ignition

David A. Reese*
Purdue University, West Lafayette, Indiana 47907
Darren M. Wright†
D2 Technology, New Castle, Delaware 19720
and
Steven F. Son*
Purdue University, West Lafayette, Indiana 47907

DOI: 10.2514/1.B34771

Fast and repeatable ignition transients for small solid rocket combustors can be difficult to achieve. This work sets out to characterize a CuO/Al thermite mixture to fill this need. Igniter function was determined using high-speed imaging, allowing an examination of product droplet size and combustion time as a function of packaging technique. Safety testing (electrostatic discharge, drop weight impact, and friction) indicated that this material is far safer than existing ignition compounds. A simple dual-criteria ignition model is applied to igniter sizing, and our modeling results were successfully evaluated using hot fire tests of motors with various exposed propellant surface conditions. The end result is a safe, inexpensive, reliable, and readily available method of igniting small (500 g–50 kg propellant mass) solid rocket combustors.

Nomenclature

a = propellant burning rate prefactor, $cm/s \cdot Mpa^n$
C = condensed phase heat capacity, $J/kg \cdot K$
$C*$ = propellant characteristic velocity, m/s
k = thermal conductivity, $W/m \cdot K$
n = propellant burning rate exponent, dimensionless
P_c = chamber pressure, Mpa
Q = heat rate, W
q = heat flux, W/cm^2
r_b = burning rate, cm/s
T = temperature, K
t = time, s
x = depth from propellant surface, cm
α = thermal diffusivity, m^2/s
ρ = propellant condensed phase density, g/cm^3

Subscripts

s = surface condition
0 = condition at infinity (initial condition)

I. Introduction

OVER the course of many small solid propellant motor firings, the need for a repeatable ignition method became apparent [1–3]. Although pyrogens and compounds such as B/KNO_3 are available, satisfactory results have been difficult to achieve over the varying sizes of motors being fired (<50 kg propellant mass). In addition, the relative lack of availability, hygroscopicity, and safety concerns regarding these compounds led to the desire to develop an igniter using widely available and inexpensive materials that would provide consistent, reliable, and safe ignition.

One of the most widely known energetic reactions is the family of thermite reactions. The concept of using thermites for motor ignition dates back at least to the 1950s, when Asp sounding rockets used in Operation Redwing were ignited with 250 g thermite charges [4]. When compared with ignition compounds in current use, thermites compare favorably with regard to energy density. They also have the benefit of being made from readily available, inexpensive, nonhygroscopic, and safe constituent materials typically found in energetics laboratories. As such, with proper formula selection, a thermite mixture may be the optimal means to ignite small-scale lab combustors.

In this work, several experiments were performed to characterize thermites for small motor ignition and determine their efficacy in this application. Standard energetic material safety tests were performed to evaluate stability of the compound under adverse conditions. To determine the most effective packaging technique, the compound was loaded into two different packages (paper and plastic) and examined during firing with high-speed imaging. A simple condensed-phase numerical model was created to determine igniter charge sizing for a range of propellant surface areas and motor port volumes, and the results evaluated using lab-scale rocket motors in BATES [5], moon, and star grain configurations.

II. Experimental Methods

A review of available thermite compounds was conducted to select candidate formulations that possess suitable energy content, reaction rate, and combustion product state. Of those available, the copper (II) oxide and aluminum system was chosen due to its high energy density, low sensitivity, reasonable gas-phase product creation, low cost, wide availability, and high reaction rate. Other thermites considered included MnO_2/Al, CuO/Mg, and Cr_2O_3/Al. The ideal stoichiometric reaction for CuO/Al proceeds as

$$3CuO + 2Al \rightarrow Al_2O_3 + 3Cu + 4\ kJ/g$$

Because the reaction begins with and results in a metallic component, the ideal heat released is simply the difference in the enthalpy of formation between the two oxides; in this case, 4 kJ/g, using data from Chase [6]. The resulting product state is over 65% condensed phase by weight. As such, the thermodynamic results from Fischer and Grubelich [7] were used to determine igniter sizing. The intense heat output and high theoretical maximum density ($5.11\ g/cm^3$) of the CuO/Al system makes it an ideal candidate for investigation. Because of the high reaction temperature, a small amount of the copper product ends in the gas phase, providing some product flow to

---

Presented as Paper 2011-5987 at the 47th AIAA/ASME/SAE/ASEE Joint Propulsion Conference & Exhibit, San Diego, California, 31 July–3 August 2012; received 23 August 2012; revision received 2 April 2013; accepted for publication 7 April 2013; published online 7 June 2013.

*School of Aeronautics and Astronautics, 500 Allison Rd.; reesed@purdue.edu.
†123 W. 7th St.; dwright@d2-tech.com.

Table 1 Propellant formulation used in test motors

Component	Wt. %
Ammonium perchlorate, 400 μm	4.0
Ammonium perchlorate, 200 μm	54.0
Ammonium perchlorate, 90 μm	4.0
Aluminum	21.0
Cr_2O_3 catalyst	0.5
HTPB binder system	16.5

Table 2 Propellant ballistic properties

Parameter	Value
a, $\mathrm{cm \cdot s^{-1} \cdot MPa^{-n}}$	0.147
n, dimensionless	0.3
$C*$ (frozen, 6.89 MPa), $\mathrm{m \cdot s^{-1}}$	1420
ρ, $\mathrm{g \cdot cm^{-3}}$	1.716

disperse the ignition energy throughout the chamber. The quantity of gas-phase product (34.3%) is small enough, however, to prevent problems from rapid depressurization or overpressurization from occurring.

Once the CuO/Al system was selected, material samples were prepared for characterization. Stoichiometric amounts of micrometric CuO (40 μm APS, Skylighter, Round Hill, VA) and Al (H15, Valimet, Stockton, CA) were weighed into a glass vial, and 20 mL of acetone was added. The thermite was mixed using a Branson S-250D digital sonifier at an 80% duty cycle for three minutes. Following mixing, the acetone was removed via vacuum oven at 40°C.

Drop weight impact, electrostatic discharge (ESD), and friction testing were accomplished in accordance with MIL-STD-1751 [8]. The ESD machine was configured using a 100 μF capacitor, allowing tests up to 2.56 J of discharge energy at 7157 V, far above the spark threshold expected from casual handling of the material. Friction testing was accomplished using a Chilworth BAM 1024 friction machine with a maximum friction loading force of 353 N.

Samples of each igniter were first fired in open air using J-Tek electric matches to evaluate action time. Each test was observed using a Vision Research Phantom v7.3 high-speed camera recording at 1000 frames per second. The results of this testing were used as a direct parameter measurement in the model developed in Sec. III.

Hot fire ignition testing of solid rocket motors with igniters sized using the model was conducted on a 2200 N capable NIST-traceable test stand, acquiring pressure and thrust data at 1000 Hz. A set of nine lab-scale rocket motors was tested to determine the effectiveness of the system. Three motors, each using one of three port geometries (BATES, moon, or star), were prepared using a standard AP-based composite propellant with the formulation listed in Table 1 and ballistic properties listed in Table 2. The grain geometries fired are illustrated in Fig. 1. All motors contained 24.8 cm of propellant length and were fired with a 0.953 cm nozzle throat. Exposed propellant surfaces (cores and ends) were carefully abraded using 100 grit sandpaper prior to firing.

III. Igniter Size Modeling

Existing igniter models from Sutton and Biblarz [9] and Barrett [10] are based on empirical data gathered from large-scale motor firings. Because this study was focused on motors with propellant masses significantly smaller than those in the existing models, a simplified theoretical approach was used to validate the large-scale empirical models prior to lab-scale testing. The ignition of a composite solid propellant consists of many exceedingly complex phenomena; the model used here, although perhaps overly simple, proved effective given the "go/no-go" requirement of motor initiation in these experiments.

Following the method of Pantoflíček and Lébr [11] and Ali et al. [12], a dual ignition criteria model was used to evaluate the energy required to initiate the motor. To ensure successful ignition, the surface temperature must be raised to the ignition temperature (critical temperature criterion), and the energy profile in the propellant must be built sufficiently to ensure that this surface temperature is maintained following igniter extinguishment (critical energy criterion). Both criteria establish an ignition time for a given energy flux; the longer of these times is considered the limiting ignition criterion and is used to size the ignition charge.

A. Development of Ignition Time Criteria

Both criteria stem from solid-phase ignition theories, in the terminology of Kulkarni et al. [13] and, thus, gas phase heat release and mass diffusion effects are neglected. To establish the minimum energy required to build the thermal wave in the propellant to the necessary thickness for sustained combustion, a Michelson preheat profile for steady burning with a thin surface reaction zone is used,

$$T(x) = (T_s - T_0)\exp\left(\frac{rbx}{\alpha}\right) + T_0 \tag{1}$$

where T_s is the surface temperature, T_0 is the initial propellant temperature, α is the propellant's thermal diffusivity, and x is the distance from the propellant burning surface. Integrating this from $x = -\infty$ to the propellant surface at $x = 0$ and multiplying by the propellant's heat capacity (here assumed constant) returns the energy in the condensed phase temperature profile Q_c,

$$Q_c = \rho C \int_{-\infty}^{0} (T_s - T_0)\exp\left(\frac{\rho C r_b x}{k}\right) \mathrm{d}x = \frac{k}{r_b}(T_s - T_0) \tag{2}$$

where $\alpha = \mathrm{k}/\rho C$, C is the condensed phase heat capacity, and k is the thermal conductivity. If the ignition charge supplies a constant energy flux of q to the surface, the critical energy ignition time is then

$$t_{\mathrm{ign}} = \frac{Q_c}{q} = \frac{k}{q r_b}(T_s - T_0) \tag{3}$$

The critical temperature ignition time is given by rearranging the classic solution for transient conduction into a semi-infinite solid [14,15] to solve for time as a function of q:

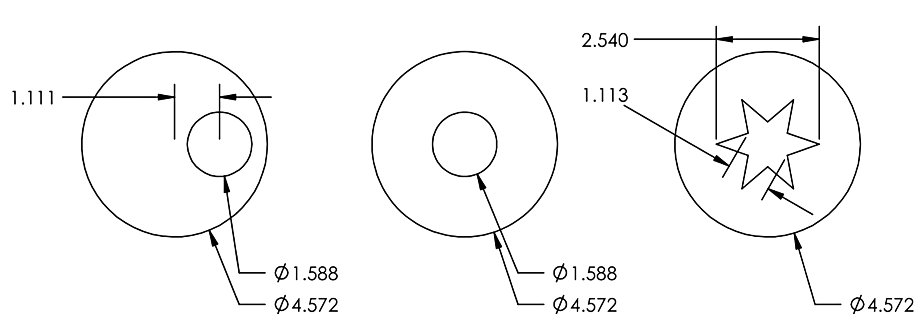

Fig. 1 End-on views of moon, BATES, and star geometries (dimensions in cm).

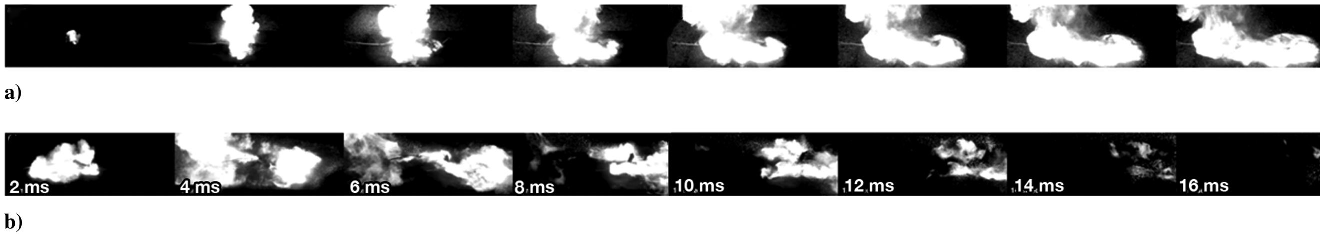

Fig. 2 Time-synchronized images of a) paper-contained and b) plastic-contained igniters.

$$t_{\mathrm{ign}} = \frac{\pi}{4\alpha}\left[\frac{(T_s - T_0)k}{q}\right]^2 \tag{4}$$

The ignition delay time t_{id} is governed by the minimum of Eqs. (3) and (4) for a given q produced by the thermite charge.

B. Determination of Charge Size

Using results from the high-speed imagery (Fig. 2), a maximum useful action time t_{act} (i.e., time during which the igniter composition is burning) of about 75 ms was determined for the thermite composition, which was nearly independent of charge mass. Thermal properties $k = 0.297\ \mathrm{W/m\cdot K}$ and $C = 1570\ \mathrm{J/kg\cdot K}$ for typical composite propellants were used in the modeling [16,17]. A Broyden–Fletcher–Goldfarb–Shanno quasi-Newton numerical solver with a cubic line search [18] was used to minimize the difference between t_{id} and t_{act} and, thus, solve the required igniter mass.

Assuming a cylindrical geometry, the output can be parameterized as a function of free port volume to enable comparison with the correlations of Sutton and Biblarz [9] and Barrett [10], mentioned earlier. The resulting plot is shown in Fig. 3a. For reasonable ignition delay times (10–50 ms), the model predicts a slightly higher igniter mass requirement than the models of Sutton and Biblarz or Barrett. These ambient pressure ignition times correspond to igniter heat fluxes between 100 and 50 $\mathrm{cal/cm^2\cdot s}$ $(4.2 - 2.1 \times 10^4\ \mathrm{W/m^2})$, in line with recommendations from Kuo [19] and others. In addition, on a log–log plot of ignition time as a function of heat flux (Fig. 3b), the expected slope of -2 is present, indicating that the limiting step for ignition is primarily the surface temperature; that is, the critical energy criterion is met before the critical temperature criterion and, thus, the temperature criterion drives the charge sizing requirement.

Because the parameter of merit for ignition is heat flux q, the surface area of the exposed propellant is of paramount concern. Portions of the igniter testing were conducted using multiple-segment BATES geometries for ease of fabrication. The challenge with such a geometry is that the ends of the grains ignite in addition to the central port and, as such, must be included in the ignition calculation. However, the ability of the thermite charge to ignite the faces of the grains quickly is somewhat doubtful because the probability of an energy-laden condensed phase particle slipping into the tight gap between grains (~1 mm) is low. As such, an amount of thermite between the "all ends lighting" and "no ends lighting" cases was taken to be the appropriate quantity for multiple segment BATES motors.

IV. Results

A. Preparation, Packaging, and Initiation

Emphasis was placed on determining the ideal method for mixing, packaging, and igniting the thermite charge inside the rocket motor. High-speed video imagery was taken of each test to determine action time for parameterization of the sizing model. Three mixing methods (hand mix dry, hand mix in acetone, sonicate in acetone) were tested in two containment methods (loose in paper, compressed in polypropylene). In addition to the choice of an electric match, ignition was also tested using an overdriven 10 Ω, 1/8 W resistor as a heat source. When driven with a high-current 24 V supply, the pyrolysis of the resistor is energetic enough to ignite pyrotechnic compounds. Yet, the resistor itself presents a significantly lower hazard of ESD initiation than a low-energy initiator, such as an electric match [20].

Examples of the two packaging methods tested are shown in Fig. 4. Testing for each method consisted of firing the charge and examining the resulting action time, condensed phase droplet size, and droplet distribution using high-speed imagery. All high-speed images were taken using a Vision Research Phantom v7 black and white high-speed camera.

The loose paper containment method was attempted first. An electric match (J-Tek, MJG Technologies, Blenheim, NJ) was able to ignite both the hand-mixed compound and the sonicated compound successfully. The resistor ignited the sonicated mixtures with ease. However, the hand-mixed compound did not fire on three out of four tries. The wet sonicated mixing processes are clearly superior for ensuring reliable ignition and, thus, were used for the remainder of testing.

The mixtures were then contained in a polypropylene sleeve, and the initiation experiments repeated. The goal of the sleeve was to tightly contain the thermite, thus increasing the burning rate. Wraps of cloth tape were used to secure the ends of the charge. During loading, the sleeve enabled the charge to be compacted to a slightly higher density than the loose paper containment method. This proved to be significant in that the higher thermal conductivity of the densified material made ignition slower using electric matches, and nearly impossible using resistors, firing one out of four tests in the

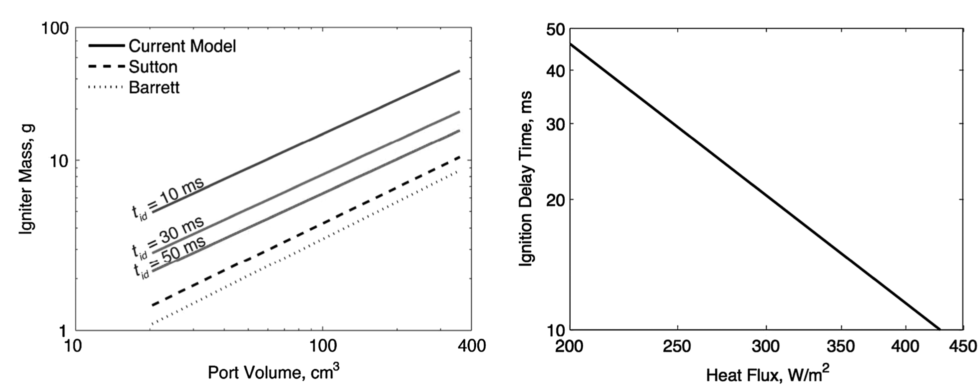

Fig. 3 Predictions for a) igniter size vs port volume, and b) t_{id} vs heat flux.

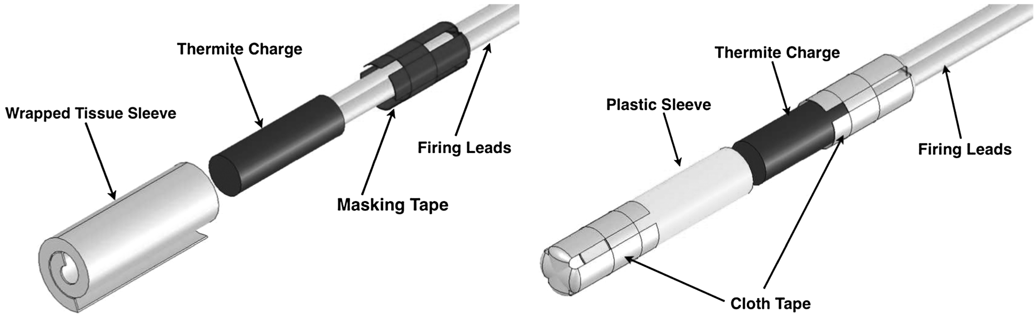

Fig. 4 Paper (left) and plastic (right) containment methods for thermite charges.

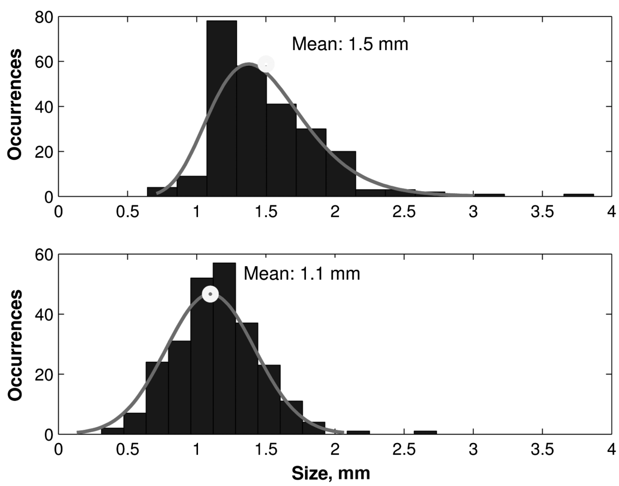

Fig. 5 Condensed phase product size distributions for paper (top) and plastic (bottom) containment techniques.

case of the latter. The mechanism for this is theorized to be simple conduction of heat away from the ignition source to the surrounding material; the paper-contained loosely packed material is not able to transport heat as quickly, thus generating a local hot spot and prompt ignition. When ignition did occur in the sleeve, the burn was significantly more violent and rapid, extinguishing 39 ms faster than the paper-contained charge.

The high-speed imagery also enabled quantitative measurements of condensed phase product droplet size. Measurements were taken directly from the still frames of the video. The results (Fig. 5) show that the plastic-contained thermite produced a higher concentration of fine droplets, an observation consistent with the faster burning rate observed in the denser compound.

Based on the results of these experiments, the igniter selected for motor testing was based on stoichiometric amounts of CuO/Al mixed via sonication under acetone, initiated by a 10 Ω resistor at 24 V and contained in a paper packet.

B. Safety Testing

To evaluate the broad ignition sensitivity of the compound, the mixed material was first subjected to a flame test, as is standard for early testing of energetic material compositions. Under a propane flame (adiabatic flame temperature >2200 K), the material would not ignite unless spread into a thin layer; the thermal conductivity of the compound thus appears to be sufficient to play a role in its ignition dynamics. With a ratio of 4.38:1 CuO:Al by mass, the thermal properties of the mixture are dominated by that of CuO ($k = 18.7\ \mathrm{W/m \cdot K}$), vs those of the Al ($k = 237\ \mathrm{W/m \cdot K}$) [21]. The importance of the thermal conductivity of the mixture was revealed during subsequent ignition method testing.

Ignition by means of ESD was of paramount concern because CuO/Al mixtures using nanoscale particles have been shown to be exceedingly sensitive to static discharge [22]. To determine sensitivity, 50 mg samples of the CuO/Al mixture under consideration were subjected to testing, with a successful ignition defined as reaction of the sample to completion. The samples were subjected to successive tests at energy levels of 0.4 mJ (93 V), 181.8 mJ (1906 V), 1137.8 mJ (4770 V), 1923.3 mJ (6262 V), and 2561.0 mJ (7157 V). Each test failed to ignite the sample.

Friction testing was also conducted on the material using a small-scale (BAM, method 1024) friction tester capable of producing up to $1.3 \times 10^8\ \mathrm{N/m^2}$ contact area. Even at this uppermost setting, no reaction was noted. Similarly, no ignitions could be obtained using the drop weight impact tester (ERL, method 1012) set at its maximum height (220 cm).

C. Hot Fire Testing

The model discussed in the preceding section was used to calculate a thermite charge ignition size for each propellant geometry. Relevant motor designations, total impulses, geometric parameters, and the resulting ignition charge sizes are listed in Table 3.

All firings proceeded nominally. Startup and peak chamber pressures $P_{c,\mathrm{init}}$ and $P_{c,\max}$ for each configuration are detailed in Table 4, along with the ignition delay time t_{id} using the definition from Sutton and Biblarz [9]. Measurement uncertainty was calculated from the tolerance of the pressure transducer, and results are reported to within tolerance. Typical pressure–time traces from each geometry are shown in Fig. 6a. The ignition pressure trace from each curve is shown in greater detail in Fig. 6b.

All motors with successful ignitions exhibited clean startup transients. The low-gas characteristic of the thermite does not obscure the motor's ignition pressure rise, as occurs in motors ignited with secondary smaller motors at the head end. This low-gas characteristic allows the collection of performance beginning immediately at

Table 4 Relevant mean data from thermite-initiated motor test firings

Motor	Initial P_c, MPa ± 0.069	Max P_c, MPa ± 0.069	t_{id}, ms ± 5
J175	2.55	2.55	6
J525	5.10	6.20	6
J820	7.65	9.03	7

Table 3 Motor designation, dimensional information, and ignition charge size

Motor	Geometry	Total impulse, N · s	Surface area, cm^2	Port volume, cm^3	Igniter mass, g
J175	Moon	1146	123.5	49.01	0.4819
J525	BATES	1113	210.1	49.01	0.8198
J820	Star	1108	248.4	52.49	0.9691

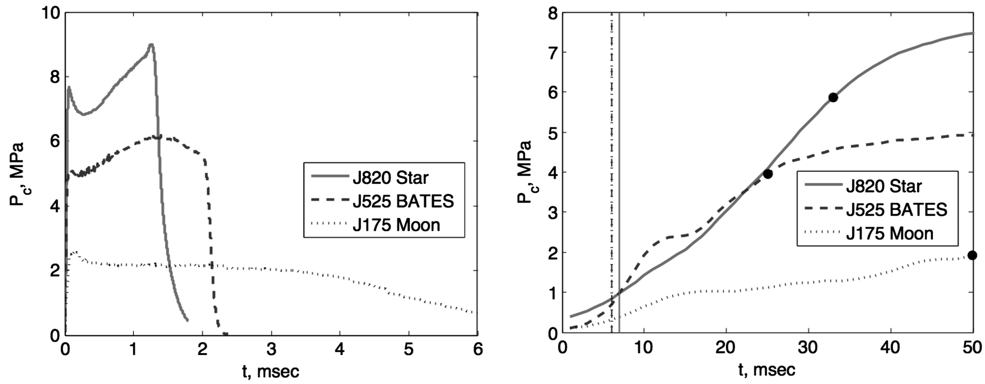

a) b)

Fig. 6 Typical a) overall and b) startup pressure traces, with t_{id} and rise time noted.

ignition, a critical phase for determining erosive effects in a combustor, for example.

The short grain length enabled some igniter compound to be ejected from the throat upon igniter firing, causing a brief delay between igniter function and propellant ignition; subsequent tests in larger motors (propellant lengths 45 cm and above) did not experience these issues. Two misfires were encountered with the moon burning grain geometries due to a lack of adequate surface preparation in the center section of the grain. The surface of these grains was reabraded with 100 grit sandpaper and subsequently ignited successfully.

Of note is the nearly identical (within measurement precision) ignition delay times in each configuration, indicating success of the sizing model. The rise time, however, varies significantly from motor to motor, likely due to exposed surface area and surface preparation quality. If ignition rise time was solely a function of exposed propellant area, the star grain, with its extremely large exposed surface, would have the lowest rise time, and the moon grain the highest. However, the BATES grain has the lowest rise time of all three geometries, likely due to the ability of each segment to be scuffed effectively prior to motor assembly. As such, both high exposed area and quality surface preparation are requirements to ensure a timely ignition.

In addition to static testing, several small sounding rocket flight tests were performed using CuO/Al for ignition, ranging in propellant mass from 700 g to 50 kg. As noted during static testing, motors with longer propellant lengths exhibited better ignition performance, likely due to the fact that the longer combustion chamber allows the thermite to react more fully before leaving the nozzle plane.

V. Conclusions

A variety of thermite systems was considered for small solid rocket motor ignition. Micron-size CuO/Al was chosen on the basis of its density, availability, safety, and high energy output. Several systems were prepared at stoichiometric ratios using different techniques to determine the most applicable mixing and packaging method. Sonicating the mixture in acetone and packaging in a loose paper sleeve created the most efficient combustion and flame spread from the thermite charge ignition.

A sizing model was developed using solid-phase ignition theory and parameterized as functions of various motor geometric variables. This model indicated that, for the high fluxes provided by the thermite igniters, the limiting criterion for composite propellant ignition in these cases is surface temperature. The resulting model compares well with existing data while demonstrating the need for slightly more compound due to the lack of chamber pressure at ignition.

This model was then used to size CuO/Al thermite igniters for lab-scale solid propellant test motors using moon, star, and multisegment BATES grain geometries. Three motors of each geometry were fired to evaluate the applicability of the model. The result was a highly consistent ignition delay across all considered geometries and peak pressures. Following ignition, the rise time to achieve pressure was governed primarily by surface preparation.

To date, several small sounding rocket flights have also been ignited using CuO/Al. These flights have used solid propellant rocket motors with propellant masses up to 50 kg, larger than most motors fired for research purposes. Based on the success of these larger flights and the motors fired in this work, CuO/Al appears to be an extremely effective means for igniting research-sized solid rocket motors.

Acknowledgments

The authors would like to acknowledge David Hailey for thrust stand assistance, and Todd Harrison and Ryan Sebastian for assistance with gathering motor test data.

References

[1] Slaby, J., Moss, J., and Heister, S. D., “Experimental Program to Assess Erosive Burning in Segmented Solid Rocket Motors,” *Proceedings of the 45th AIAA/ASME/SAE/ASEE Joint Propulsion Conference*, Denver, CO, AIAA Paper 2009-5176, 2009.

[2] Rettenmaier, A. K., and Heister, S. D., “Experimental Evaluation of Erosive Burning in Planar Combustor,” *Proceedings of the 47th AIAA/ASME/SAE/ASEE Joint Propulsion Conference*, Diego, CA, AIAA Paper 2011-5564, 2011.

[3] Kittell, D., Pourpoint, T. L., and Son, S. F., “Further Development of an Aluminum and Water Solid Rocket Propellant,” *Proceedings of the 47th AIAA/ASME/SAE/ASEE Joint Propulsion Conference*, San Diego, CA, AIAA Paper 2011-6137, 2011.

[4] Morrow, R. B., and Pines, M. S., *Small Sounding Rockets: A Historical Review of Meterological Systems, 1955 to 1973*, Small Rocket Press, Searingtown, New York, 2000, pp. 73–78.

[5] Geisler, R. L., and Beckman, C. W., “The History of the BATES Motors at the Air Force Rocket Propulsion Laboratory,” *Proceedings of the 34th AIAA/ASME/SAE/ASEE Joint Propulsion Conference*, Cleveland, OH, AIAA Paper 98-3981, 1998.

[6] Chase, M. W. J., “NIST-JANAF Thermochemical Tables, 4th ed.,” *Journal of Physical and Chemical Reference Data, Monograph 9*, Springer-Verlag, Seacaucus, New Jersey, 1998, pp. 1–1951.

[7] Fischer, S. H., and Grubelich, M. C., “A Survey of Combustible Metals, Thermites, and Intermetallics for Pyrotechnic Applications,” *Proceedings of the 32nd AIAA/ASME/SAE/ASEE Joint Propulsion Conference*, AIAA, Lake Buena Vista, FL, AIAA Paper 1996-3018, 1996.

[8] Indian Head Division, Naval Surface Warfare Center, “Safety and Performance Tests for the Qualification of Explosives (High Explosives, Propellants, and Pyrotechnics),” U.S. Department of Defense, MIL-STD-1751A, Dec. 2001.

[9] Sutton, G. P., and Biblarz, O., *Rocket Propulsion Elements*, 7th ed., Wiley, New York, 2001, pp. 563–568.

[10] Barrett, D. H., “Solid Rocket Motor Igniters,” NASA SP-8051, 1971.

[11] Pantoflíček, J., and Lébr, F., “Comments on ‘Surface Exotherm Reaction During Ignition of Ammonium Perchlorate Propellants’,” *AIAA Journal*, Vol. 6, No. 7, 1968, pp. 1435–1436. doi:10.2514/3.55404

[12] Ali, A. N., Son, S. F., Asay, B. W., and Decroix, M. E., "High-Irradiance Laser Ignition of Explosives," *Combustion Science and Technology*, Vol. 175, No. 8, 2003, pp. 1551–1571.
doi:10.1080/00102200302358

[13] Kulkarni, A. K., Kumar, M., and Kuo, K. K., "Review of Solid Propellant Ignition Studies," *AIAA Journal*, Vol. 20, No. 2, 1982, pp. 243–244.
doi:10.2514/3.51071

[14] Carslaw, H., and Jaeger, J. C., *Conduction of Heat in Solids*, Clarendon Press, Oxford, 1959, pp. 188–213.

[15] Incroprera, F. P., and DeWitt, D. P., *Introduction to Heat Transfer*, Wiley, New York, 1985, pp. 149–150.

[16] Selzer, H., "The Temperature Profile Beneath the Burning Surface of a Composite Ammonium Perchlorate Propellant," *Symposium (International) on Combustion*, Vol. 11, No. 1, 1967, pp. 439–446.
doi:10.1016/S0082-0784(67)80168-1

[17] Alavilli, P., Buckmaster, J., Jackson, T. L., and Short, M., "Ignition Transient Modeling for Solid Propellant Rocket Motors," *Proceedings of the 36th AIAA/ASME/SAE/ASEE Joint Propulsion Conference*, Huntsville, AL, AIAA Paper 2000-3567, 2000.

[18] Broyden, G. C., "The Convergence of a Class of Double-Rank Minimization Algorithms," *Journal of the Institute of Mathematics and its Applications*, Vol. 6, No. 3, 1970, pp. 76–90.
doi:10.1093/imamat/6.3.222

[19] Kuo, K. K., "Ignition and Unsteady Combustion of Solid Propellant," Lecture Series No. 180, AGARD, Saint-Médard-en-Jalles, France, Sept. 1991, p. 119.

[20] Dahlquist, R., "The Dahlquist Resistor Igniter," Tech. Rept., Aerocon Systems, San Jose, California, 1998.

[21] Weast, R. C. ed., *Handbook of Chemistry and Physics*, 56th ed., CRC Press, Boca Raton, FL, 1975, 4-44–4-62.

[22] Foley, T., Pacheco, A., Malachi, J., Yetter, R., and Higa, K., "Development of Nanothermite Composites with Variable Electrostatic Discharge Ignition Thresholds," *Propellants, Explosives, Pyrotechnics*, Vol. 32, No. 6, 2007, pp. 431–434.
doi:10.1002/prep.200700273

J. Seitzman
Associate Editor